Semiconductor Optical Space Switches

M. Renaud, M. Bachmann, and M. Erman, *Member, IEEE*

(Invited Paper)

***Abstract*—This paper reviews the various optical space switch structures on III–V semiconductor material. Their characteristics are discussed in the context of optical transport and switching network applications exploiting wavelength division multiplexing.**

I. Introduction

CURRENT evolution of optical networks is going toward wavelength division multiplexed (WDM) networks based on optical add and drop multiplexers (OADM's) and optical crossconnects (OXC's) for routing the WDM signals. In a later stage, the inclusion of optical packet switching is also foreseen.

For all these applications, though many different architectures can be implemented, a space stage is likely to be used in most of them and therefore optical space switches are expected to play an important role in future broadband optical networks. Examples of an OADM, an OXC and an optical packet switching fabric presented respectively in Figs. 1–3 identify the use of the space switches.

Fig. 1 shows the general architecture of an OADM. A prototype OADM has been designed for 4 wavelength channels, each supporting STM-16 (2.5-Gb/s) capacity [1]. Already commercially available components such as tunable Fabry–Perot filters, optomechanical switches and 3-R optoelectronic regenerators have been used to build the demonstrator. Three nodes were interconnected in a unidirectional self-healing two-fiber ring network demonstrator. Nodes are separated by 90 km of standard single mode fiber.

Performance evaluation of the demonstration used $2^{23}-1$ pseudorandom bit sequences and 103 possible configurations were successfully tested over long periods of time (more than 66 h), proving the overall system reliability. By circulating a signal four times in the loop, and changing the wavelength at each node, it was possible to simulate the cascade of 12 nodes along a 1080-km path and a BER better than 10^{-15} had been achieved [1].

The use of commercially available components shows that early implementation of OADM's is technically feasible. More advanced components as discussed below will further improve the overall performance, in particular the reconfiguration time.

WDM cross-connects can range from fixed WDM cross-connects to wavelength interchanging cross-connects thus offering different functionalities. The full functionality always requires a combination of space switches, wavelength selective elements (demultiplexers or filters) and wavelength converters. These elementary blocks can be arranged in different ways. For instance, one can use the following sequence: wavelength demultiplexing, space switching, wavelength conversion and wavelength multiplexing [2].

Fig. 2 schematically illustrates an arrangement that can be referred to broadcast and select [3]. In addition to fully nonblocking, broadcasting and multicasting, this configuration offers the advantage of requiring elementary switching matrices of reduced size only. It uses advanced optoelectronic components, in particular for the space switching stage (gain clamped semiconductor optical amplifiers, see Section IV) and the wavelength conversion stage (all optical semiconductor wavelength converter). In a sparsely equipped demonstration, a cascade of two 4×4, eight wavelength crossconnects has been tested over 320 km of standard single mode fiber. Error-free operation (BER of 10^{-15}) was successfully demonstrated at 10 Gb/s [4].

In contrast to OXC, the switching matrices of an optical packet cross-connect has to reconfigure synchronously with the packet flow, within a reconfiguration time which needs to be as small as possible (typically ns) so as to minimize the guard time to be introduced between different packets. In addition, the contention problem, which arises when two packets want to reach the same address simultaneously, has to be solved. This requires optical memory allowing to delay packets by a multiple of the packet duration. The demonstrator architecture is depicted in Fig. 3.

The architecture relies on the use of wavelength encoding and selection [5]. It shares several principles with the OXC broadcast and select architecture described above. The additional features are essentially the reconfiguration speed and the optical delay lines. The delay lines consist of length-calibrated optical fibers. All the other components use again advanced optoelectronic components, all based on various combinations of semiconductor optical amplifiers, which allows reconfiguration times below 1 ns.

Experimental results have shown the feasibility of 16×16 switching matrices at bit rates up to 10 Gb/s with limited sensitivity penalties [6]. Recently, the operation with 16-channel WDM signals in the 1530–1560-nm wavelength range has been demonstrated in a subequipped matrix (2×1 representative of a 16×16 broadcast and select switching matrix).

Several demonstrations of space switches, already at a relatively large scale have been made using mature technologies.

Manuscript received October 29, 1996; revised November 11, 1996. This work was supported in part by the European Commission. Part of the work was carried out within the European projects RACE ATMOS, ACTS KEOPS and ACTS OPEN.

The authors are with Alcatel Alsthom Corporate Research Centre, c/o Alcatel Alsthom Recherche, 91460 Marcoussis, France.

Publisher Item Identifier S 1077-260X(96)09510-X.

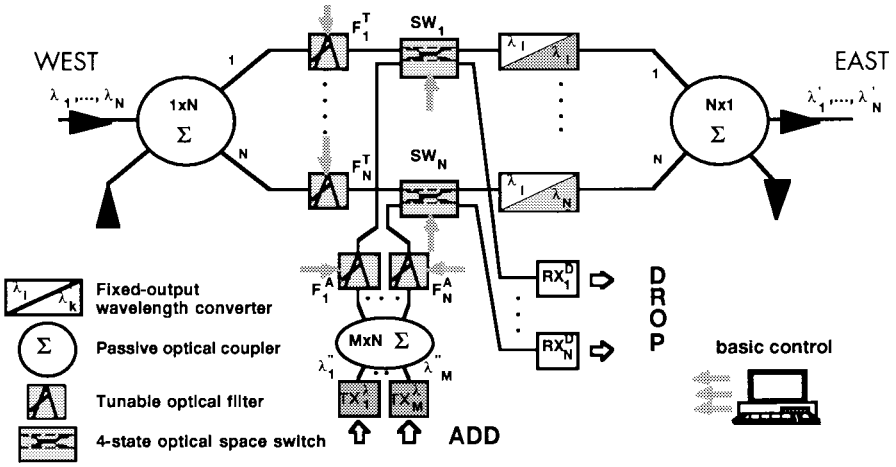

Fig. 1. Architecture of multiwavelength optical add–drop multiplexer [1].

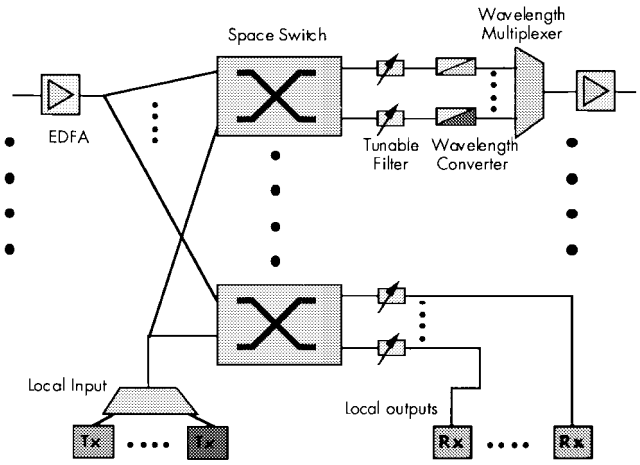

Fig. 2. Architecture of multiwavelength optical cross-connect [3].

Hence, a strictly non blocking 512 × 512 optical fiber switch based on three-stage Clos network has been demonstrated with connector type optical switches [7]. However, new solutions aiming at combining simultaneously reliability, compactness, higher switching speed and cost effectiveness have to be used for massive application.

The requirements for the space switches will be system dependent but preferably the space switches should feature the following:

- polarization independence;
- low crosstalk;
- low-insertion loss or even gain;
- wavelength independence (in the EDFA wavelength range);
- multiwavelengh operation;
- bit-rate transparency (up to at least 10 Gb/s);
- fast switching;
- simple implementation;
- scalability.

During the last decade, integrated optics space switches have been investigated on $LiNbO_3$ [8]–[11], SiO_2 [12], polymers [13]–[14] and III–V semiconductors [see following sections]. The problem of coherent crosstalk as recently highlighted in system experiments [15] pushes the requirement on crosstalk to very low values which will naturally exclude some switch options. The stability of characteristics under an electric field remains critical for $LiNbO_3$ and electrooptic polymers. Recently, stable operation of a polymer switch has been reported with thermo-optic operation [13]. Thermooptic effect is, however, slow and limits the switching speed of the devices.

In this paper, we will concentrate on semiconductor space switches (mainly on InP) which appear today as an attractive solution. Both, electrooptic space switches of several types (directional couplers, Mach–Zehnder interferometers, digital optical switches) and optical amplifier gates will be reviewed and discussed in terms of important parameters such as crosstalk, insertion losses, polarization and wavelength dependence, and switching speed. Technological issues will also be addressed.

II. Basic Switching Principles

Physical properties and processing flexibility make semiconductor materials very suitable for guided wave devices. Multilayer structures that can be grown by sophisticated epitaxial techniques in combination with processing techniques that are common to semiconductor industry give semiconductor devices large design freedom.

The double heterostructure waveguide, where the optical confinement is achieved by a compositional change, is now the most often used waveguide structure on semiconductor material. In the InP material system, the core waveguide and cladding layers are usually InGaAsP and InP, respectively. The double heterostructure allows to optimize separately the optical and the electrical waveguide structure, an important advantage as compared to homojunction structures. Lateral confinement is usually achieved by localized etching. In the case of buried waveguides, the core layer itself is etched [16]. Etching of the cladding layers results in rib waveguides [17]. Deep ridge structures are formed by etching both, cladding and core layers [18]. The quality of the epitaxial layers as well as the overall processing has been improved considerably over the past years. As a result, semiconductor waveguides with losses as low as 0.2 dB/cm, similar to the results reported on

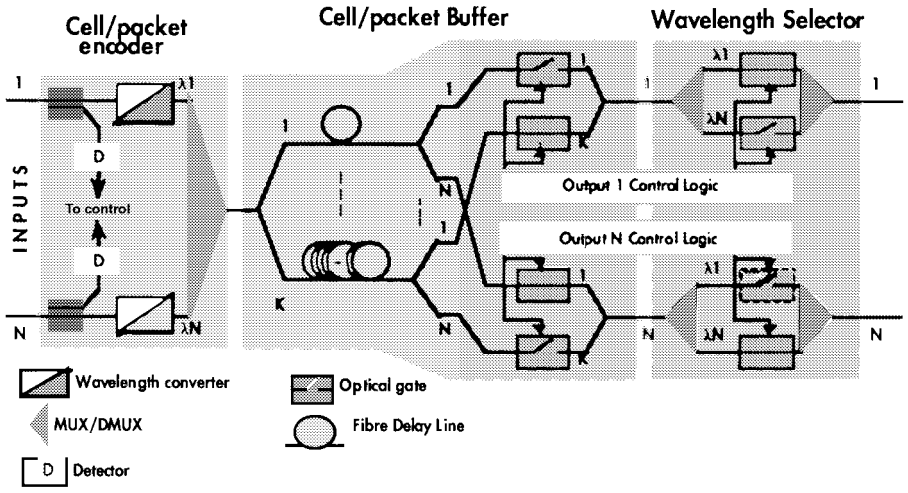

Fig. 3. Architecture of optical packet cross-connect [5].

$LiNbO_3$ waveguides, have been obtained for the embedded [19] and the rib waveguides [20]. Even with the presence of the p contacting layer and electrodes, the losses can remain below 1 dB/cm.

In semiconductor waveguide devices, a large number of physical effects allows to modulate either the index of refraction or the absorption/gain. The index of refraction itself can be modulated electrically by applying an electric field, or by injecting carriers. In the presence of an electric field, the semiconductors exhibit the linear electrooptic effect (like $LiNbO_3$), as well as the quadratic Kerr effect [21]. Although the electrooptic coefficient for semiconductors is smaller than that for $LiNbO_3$, the electrooptic modulation in semiconductors is at the same level as in $LiNbO_3$ thanks to the index change variation being proportional to the third power of the refractive index (3.2 for InP and 1.5 for $LiNbO_3$). Close to the band edge, the electrooptic effect can considerably be enhanced by the Franz–Keldysh effect in bulk materials [49]. If the waveguide includes quantum wells, quantum confined Stark effect (QCSE) will occur in the presence of an electric field [22]. This often polarization dependent effect can be made polarization independent with appropriate strain in InGaAsP–InP MQW's [23] or with wide-well InGaAlAs–InAlAs MQW's [18]. A more serious drawback of the QCSE is the strong wavelength dependence, which makes quantum-well devices less attractive for building large switching matrices with requirements discussed in the introduction.

The index of refraction of semiconductors is changed by free carriers due to different effects such as plasma resonance, bandfilling and band shrinkage [24]. The index modulation via carrier injection can be very strong: an index change of 0.1 can be achieved for both TE and TM modes, which is two orders of magnitude higher than the modulation via the electrooptic effect. The drawback of the carrier injection type devices as compared to the electrooptic ones is the lower speed being limited by carrier recombination times. Waveguide structures that combine both, the electrooptic modulation and carrier modulation, have been made with a doped core InGaAsP that can be depleted when the waveguide is reverse biased [25].

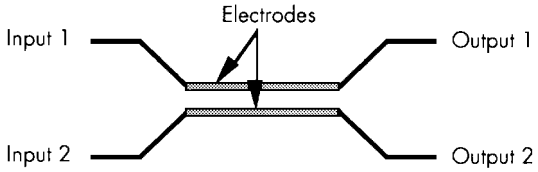

Fig. 4. Schematic view of a directional coupler.

This structure has the advantages of exhibiting about three times larger modulation as compared to electrooptic devices, a nearly similar modulation for TE and TM modes, and a speed that is limited by device capacitance rather than carrier recombination time [26]. In addition, carrier injection can be used for changing the absorption of the material, and in the vicinity of the band gap, for providing optical gain.

A number of guided wave devices that take advantage of the above-mentioned modulation principles have already been demonstrated and are reviewed in the following sections. They include interferometric devices such as directional couplers and Mach–Zehnder interferometers, mode transformers such as digital optical switches and semiconductor optical amplifiers.

III. Space Switches Exploiting Electrooptic Effect

A. Directional Couplers

Directional couplers (DC) [27] consist of two coupled waveguides (Fig. 4). They are characterized by their coupling length (Lc) and the bias voltage or current to achieve a π phase shift in the interferometer. The coupling length is usually different for TE and TM modes and varies rapidly with geometrical parameters which implies tight fabrication tolerances. As the switch response is not digital, a precise control of the biasing conditions can be required.

Directional couplers only require small index changes and can therefore be fabricated either with electrooptic, carrier depletion or carrier injection waveguides.

Example of the response curve of a carrier depletion directional coupler [28] is given in Fig. 5 where the switching voltage is only 11 V for a 2-mm-long device and crosstalk

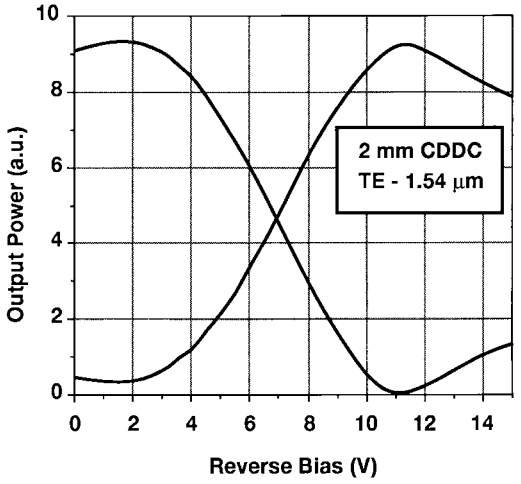

Fig. 5. Switching response of a 2-mm-long carrier depletion directional coupler [28].

is close to −20 dB in the switched state and −15 dB in the off state.

To avoid a precise control of the coupling length of the DC, $\Delta\beta$ devices have often been preferred [29]–[31]. This configuration, which requires a length between Lc and 3Lc and 3 isolated electrodes allows to adjust electrically the cross and bar states.

Directional coupler based monolithically integrated 4 × 4 space switch matrices have been fabricated on InP with a complexity of five carrier injection switches [32], six carrier injection switches [29] and 16 electrooptic switches [30]. These devices exhibit crosstalk in the 10–15-dB range for TE polarization and chip losses in the order of 15 dB. To cope with fabrication tolerances, stop etch layers can be introduced to precisely control the etch depth [32]. A 4 × 4 switch matrix, which uses the QCSE of InGaAlAs–InAlAs MQW structures and working in TE mode with crosstalk below −17 dB was also reported in a rearrangeable nonblocking Benes network built with 6 switches [33]. Size up to 8 × 8 has been demonstrated on GaAs [31] with 64 monolithically integrated switches. Thanks to highly confined waveguides, the whole device is only 26.5-mm long and chip losses are maintained at a value as low as 8.7 dB by using an appropriate smooth etching process.

The moderate crosstalk of the DC structure can considerably be improved to the −30 to −40 dB range by cascading two devices [34]. However, the resulting large size limits the switch matrix size complexity.

A selection of realized DC space switches is summarized in Table I.

The above-described directional coupler arrangement was historically the first to be used for integrated optic waveguide switches. This type of switch has some drawbacks, however. Manufacturing control of the coupling length is difficult and switches are polarization sensitive: serious limitations in particular for semiconductors for practical applications. Directional coupler switches are polarization dependent for two reasons: the coupling length is usually different for TE and TM modes and the electrooptic effect used for refractive-index changes can be polarization dependent. It is difficult, but not impossible [35], to overcome this limitation since mode coupling and refractive index change take place at the same location.

TABLE I
A SELECTION OF PUBLISHED DC SPACE SWITCHES ON III–V SEMICONDUCTOR

Matrix Type	Switch points	Material	Results	Ref / year
4x4	5 CIDC	InGaAsP	TE, crosstalk ≤ - 10 dB, insertion loss < 15 dB, switching > 10 mA, size 6.5 mm	[32] 1992
4x4	6 CIDC	InGaAsP	TE, crosstalk ≤ - 15 dB, chip loss 15 dB, switching ~ 10 mA, size 35 mm	[29] 1991
4x4	16 EODC	InGaAsP	TE, crosstalk ≤ - 10 dB, propagation loss 3 dB/cm, switching < 30 V, size 35 - 40 mm	[30] 1991
4x4, Benes	6 QCSE DC	InGaAlAs MQW	TE, crosstalk ≤ - 15 dB, 18 dB chip loss, switching < 6 V, size 9 mm	[33] 1993
8x8	64 EODC	GaAs/ AlGaAs	TE, crosstalk ≤ - 21 dB, 8.7 dB chip loss, switching < 25V, size 26.5mm	[31] 1992

CI: Carrier injection. EO: Electrooptic. QCSE: Quantum-confined Stark effect.

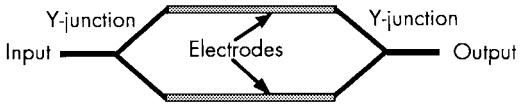

Fig. 6. Integrated optical Mach–Zehnder interferometer.

B. Mach–Zehnder Interferometric Switches

An important advantage of the Mach–Zehnder Interferometer (MZI) switches as compared to directional couplers is the geometrical separation of mode-coupling and phase-shifting regions. Independent optimization is now possible.

The operation principle of a MZI is as follows: Input light is divided by a first beam splitter into two light beams. The two light beams then follow different paths and are merged at the second beam splitter, where the two beams interfere. The interference depends on the relative phase (cosine like behavior).

MZI's have very early been used for integrated optical switches [36]–[38]. An example on GaAs as shown in Fig. 6 used Y-junctions as beam splitters and combiners [39]. An electric field applied to one or both of the waveguides between the Y-junctions changes the refractive index, which changes the relative phase at the combining Y-junction. Destructive interference at the output means, that the first-order mode in the output waveguide is excited. To achieve a high extinction ratio, it is important that this first-order mode is not guided.

In contrast to the above MZI modulators, space switches need two selectable outputs. The combining element in above examples, the 2 × 1 Y-junction, must therefore be replaced by a 2 × 2 mode coupler as shown in Fig. 7. Directional couplers as well as multimode interference (MMI) couplers have been used. For polarization-insensitive MZI switches, not only the previously discussed phase shifters, but also the 2 × 2 couplers must be polarization insensitive. Thus MMI couplers are often used to take advantage of their polarization-insensitive characteristics and fabrication tolerances [40], [41]. MMI couplers are regions of the integrated optical waveguide devices which can support a multitude of guided modes. The

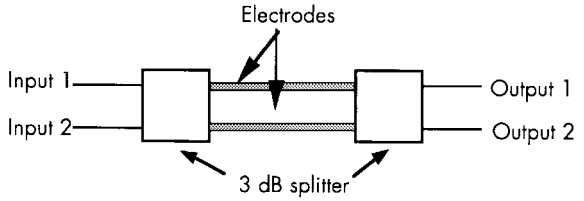

Fig. 7. Integrated optical Mach–Zehnder interferometer space switch with two inputs and two outputs.

propagation constants of these modes are such, that after a certain propagation length, the phases modulo 2π are equal for all propagated modes. This means, that the light distribution at the input of the MMI coupler is reproduced after that distance, thus, forming self-images. MMI couplers cannot only be used for reproduction of light distributions, but they can also form multiple self-images at shorter device lengths [42]–[44].

To achieve polarization-insensitive phase shifts while using fast electrooptic field effects in bulk InGaAsP–InP materials, specially oriented phase-shifting waveguides have been applied [45], [40]. Recently, such type of switches have been used to form a matrix arrangement with four input and four output fibers. Mode adaptors allowed for low fiber-chip coupling losses and relaxed alignment tolerances [46]. Optimizations resulted in record low fiber-to-fiber losses of 5 dB [47], while maintaining polarization insensitive operation. On–off ratios in the 1.53–1.56-μm wavelength range exceed 15 dB for switching voltages of 4.5 V. Thanks to the exploitation of electric field effects, 200-ps switching times have been reported.

Besides work based on bulk InGaAsP material, 2×2 MZI switches using polarization independent electrooptic effects in MQW structures have been reported [18], [23], [48]. Again, MMI couplers are used as splitters and combiners. Low switching voltages in the range of 5 V for short, submillimeter electrode lengths have been achieved. High efficiency is often obtained by working close to the bandedge of the MQW-stack which results in high loss and a strong wavelength dependence of the switching voltages. Application for WDM signals becomes difficult.

MZI's are well suited for high-speed application, since electrooptic field effects can be exploited. Traveling-wave electrodes integrated on bulk InGaAsP–InP MZI switches allowed a bandwidth of 35 GHz [49].

In addition to the well-known 2×2 MZI switches, $N \times N$ MZI switches have been proposed [41] and realized on GaAs [50] as well as on InP [51] demonstrating polarization insensitive switching.

Table II summarizes a selection of published results using MZI switches.

TABLE II
A SELECTION OF PUBLISHED MZI SPACE SWITCHES ON III–V SEMICONDUCTOR

Matrix Type	Switch points	Material	Results	Ref / year
2x2	QSCE MZI	InGaAs MQW	TE & TM, crosstalk ≤ -10 dB, insertion loss 20 dB, switching 4.5V electrode 675 μm, size 1.84 mm	[23] 1992
2x2	EO MZI	InGaAsP	TE & TM, crosstalk ≤ -16 dB, on-chip loss < 3.2 dB, switching 6 V electrode 3 mm, size 7 mm	[40] 1993
2x2	EO MZI	InGaAsP	TE, crosstalk ≤ -12 dB, loss 1.5 dB/cm, switching 6 V electrode 3 mm, bandwidth 35 GHz	[49] 1994
2x2	QSCE MZI	InGaAsP MQW	TE, crosstalk ≤ -15 dB, insertion loss 22 dB, switching 6.8V electrode 0.5mm, bandwidth 10GHz	[48] 1995
2x2	QSCE MZI	InGaAlAs MQW	TE & TM, crosstalk ≤ -20 dB, insertion loss 14 dB, switching 4.5V electrode 1.5 mm, size 4 mm	[18] 1996
2x4 module	4 EO MZI	InGaAsP	TE & TM ±0.5 dB, crosstalk ≤ -10 dB insertion loss 12 dB, switching 5.5V electrode 6 mm, switch time 200 ps	[46] 1994
4x4 module	4 EO MZI	InGaAsP	TE & TM ±0.5 dB, crosstalk ≤ -15 dB insertion loss 5 dB, switching 4.5 V electrode 6 mm, switch time 200 ps, optical badnwidth >30 nm	[47] 1996

EO: Electrooptic. QCSE: Quantum-confined Stark effect.

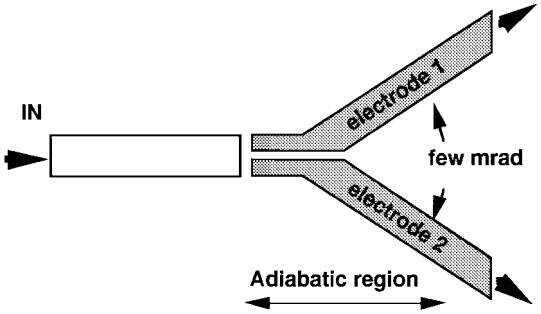

Fig. 8. Schematic view of a digital optical switch.

C. Digital Optical Switches

The digital optical switch (DOS) as shown in Fig. 8 is based on adiabatic mode evolution [52] in contrast to directional couplers and Mach–Zehnder interferometers that use interference effects. Consequently, polarization independent operation can be obtained for DOS thanks to its digital response. Moreover, this behavior allows large optical bandwidth of more than 50 nm in both TE and TM polarizations [53]. The required refractive index change for switching is higher than for DC and MZI but still relatively small (<0.003) if the angle of the Y-junction is small (several milliradians). Thus, the switching of the DOS can be obtained both by reverse- or forward-bias operation in a p-i-n heterostructure [54], [55] but cannot be obtained with pure electrooptic effect in bulk material. Thanks to the Y-junction shape, the DOS acts as a 3-dB splitter when no bias is applied, and provides easily the broadcasting function which is needed in many system applications. Also, the digital response allows relaxed bias control.

First devices reported on InP made with single core waveguide structure exhibit switching current as small as 6 mA (Fig. 9) and around -10 V in carrier depletion with a crosstalk <-15 dB for 5-mm-long electrodes and 3-mrad angle.

As light is switched into the arm with the highest refractive index, it goes into the biased arm under reverse bias and into the opposit arm under forward bias. In the depletion operation, this leads to a tradeoff between low crosstalk and reasonably low losses introduced by electroabsorption at high voltage. The current injection operation mode does not present this limitation and is preferred. In push–pull operation, carrier injection and carrier depletion are combined and complete switching with crosstalk < -15 dB is obtained for only $+1.8$ V on one electrode and -1.8 V on the opposit electrode [55]. This push–pull mode allows high-speed operation in the Gb/s

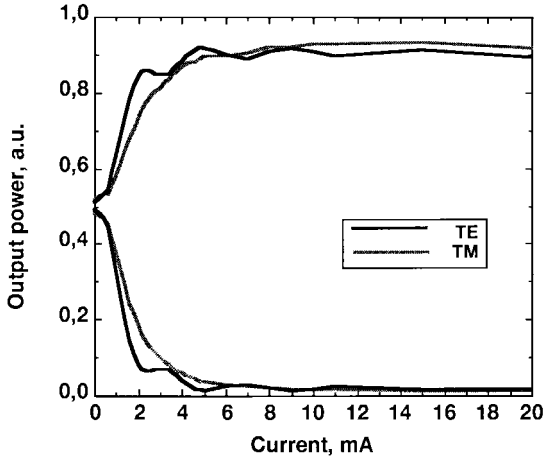

Fig. 9. Typical switching response curve of a DOS in current injection [53].

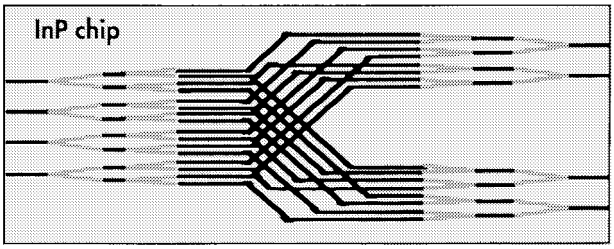

Fig. 10. Architecture of monolithically integrated 4 × 4 DOS InP switch matrix with 24 DOS and 32 mirrors [57].

range. 1 × 4 and 4 × 4 [56] switching matrices have been reported with these technologies in a strictly nonblocking tree architecture with 24 DOS.

To reduce the size of the 4 × 4 DOS switch matrix configuration, DOS have been monolithically integrated with mirrors [57]. The interconnection shuffle is then achieved in about 1 mm. The total length is reduced from 40 to 20 mm (Fig. 10).

In addition, a triple-core waveguide has been introduced to get waveguides with larger modes compatible with fiber/chip coupling losses as low as 1 dB/facet. 1 × 4 and 4 × 4 DOS switching matrices have been packaged (Fig. 11) and used in cross-connect system environment to switch 10-Gb/s data streams [58].

High-speed compact DOS with MQW structures [59] were also reported with a 3-dB optical bandwidth of 10 GHz. However, these structures exhibit relatively high-propagation losses (12.5 dB/cm) and are polarization dependent, which makes them not practical for large switch matrix applications.

The coherent crosstalk as highlighted recently [15], pushes the requirement in crosstalk of the space switches to −30 to −40 dB. Though single 1 × 2 DOS with −30-dB crosstalk have been reported on InP [60], structures compatible with large switching matrices (i.e., compact, integrable and compatible with low multifiber/chip coupling losses) have only demonstrated polarization independent crosstalk up to −20 dB. These results have been obtained with compact DOS structures (electrode length of 1.5 mm) on triple core structures and integration has been demonstrated on a 2 × 2 tree

Fig. 11. Packaged 4 × 4 DOS InP switch matrix.

TABLE III
A SELECTION OF PUBLISHED DOS SPACE SWITCHES ON III–V SEMICONDUCTOR

Matrix Type	Switch points	Material	Results	Ref / year
1x2	CDDOS	InGaAsP	crosstalk <-14 dB for TE & TM, switching -12 V, > 50 nm optical bandwidth, 5 mm, < 2 dB/cm	[54] 1991
4x4	24 CIDOS	InGaAsP	crosstalk <-16 dB per DOS for TE & TM, 25 dB fibre to fibre loss, switching < 10 mA, size 40 mm, optical bandwidth > 50 nm	[56] 1992
4x4	24 CIDOS	InGaAsP triple core	crosstalk <-13 dB per DOS for TE & TM, 15 dB fibre to fibre loss, switching < 30 mA, size 20 mm, optical bandwidth > 50 nm	[57] 1993
1x2	CIDOS	InGaAsP	crosstalk <-20 dB for TE & TM (best -30 dB),switching 50/100 mA for 1.3/1.5 μm, 200 nm optical bandwidth, 3 mm electrode, 2dB/cm	[60] 1994
1x2	QCSEDOS	InGaAsP	TE, crosstalk ≤ - 7 dB, 1.25 dB chip loss, switching - 4 V, size 0.9 mm, 10 GHz 3 dB bandwidth	[59] 1995
1x2	CIDOS	InGaAsP triple core	crosstalk < 18 dB in TE & TM, switching 30 mA, 1.5 mm electrode, 10 dB f to f loss for a 2x2 matrix	[61] 1995

architecture with about 10-dB insertion losses in a packaged module [61]. More recently, further crosstalk improvement has been proposed [62] and tolerant designs has been given to achieve −30-dB crosstalk for both polarizations over a 150-nm wavelength range by introducing a single electrode mode converter and tapered electrodes [63].

Fig. 12 shows a switching curve of an InP-based DOS with integrated mode converter that achieves crosstalks in the −30-dB range.

Selected results on DOS matrices are given in Table III.

IV. ACTIVE SPACE SWITCHES

Current injection into semiconductor pn-junctions generates free carriers. This carrier modulation varies the loss and/or gain characteristics. Employing these characteristics, switchable semiconductor optical amplifiers (SOA's) can be realized. Many different configurations for the different applications have been demonstrated. For an overview, see, for example, [64] and references therein. Here, we are interested in the use of such gain modulators for space switching applications. Most often, the tree structure as shown in Fig. 13 is used.

A fully connected shuffle network between input and output ports is realized using adequate power splitters and combiners. Each connecting path can be switched on or off using the

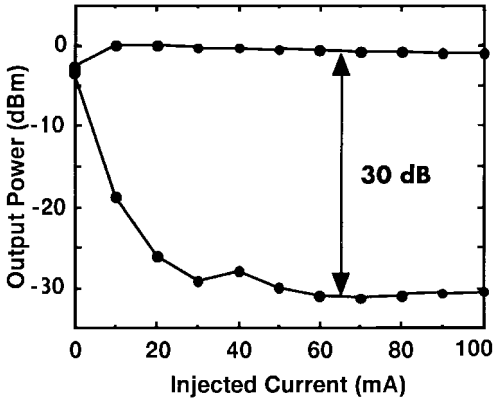

Fig. 12. InP-based DOS with integrated mode-converter achieves low crosstalk in the −30-dB range for TE polarization.

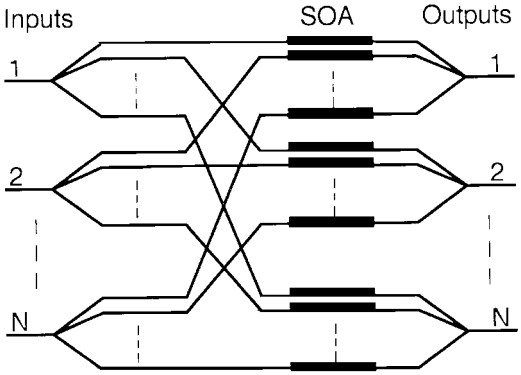

Fig. 13. SOA-based $N \times N$ space switch in a tree arrangement.

corresponding SOA. $N \times N$ SOA's are therefore required. Such a switching matrix inherently generates splitting losses that can be important for large switch arrays. To compensate for the losses, additional booster amplifiers can be included with the drawback of noise accumulation. The configuration of Fig. 13 forms a strictly nonblocking space switch with broadcast capabilities.

Several research groups have demonstrated monolithically integrated 2 × 2 switches [65]–[69] or 1 × 4 switches [70] on InP semiconductor with various performances. All devices use monolithically integrated active and passive waveguides. Switches use SOA's designed for single polarization operation [65], [68], [70] or for polarization insensitivity [67], [69]. Integrated 2 × 2 switches including lasers have also been reported [66]. Net fiber to fiber gains for all paths using a single stage of SOA's have been reported in [67], [69]. On–off ratios up to 45 dB are feasible [67].

Fully integrated 4 × 4 switches required two additional booster stages to achieve nearly zero loss performances in a polarization dependent [71] as well as in a polarization insensitive configuration [72] for wavelengths around 1.55 μm. Such 4 × 4 matrices have successfully been tested in system experiments [73], [74]. A different approach using 4 × 4 Benes configuration has given zero loss performances at 0.9-μm wavelength [75].

If the broadcasting capability is not required, it is most advantagous, if splitting and combining losses can be avoided. This is possible with the single-slip-structure (S3), where total

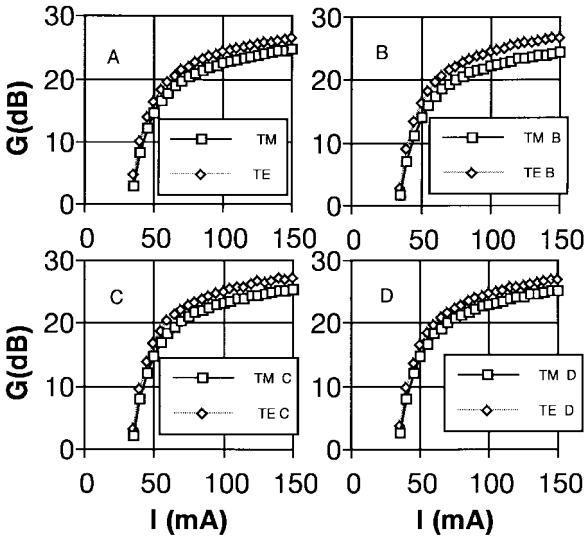

Fig. 14. Uniform gain of SOA array [81].

internal reflection (TIR) switches are added in order to switch the "3-dB-couplers". Lossless 2 × 2 [76] or even 4 × 4 switches with gain [77] have already been reported for 1.3-μm operating wavelength.

A complementary approach to the monolithic integration is the hybrid integration of the SOA's on substrates including very low loss passive waveguides. The most successful solution is probably to integrate not single SOA's but larger quantities in the form of multichannel SOA-arrays. Early integration of two 8-SOA arrays operating at 1.3-μm wavelength on a silica-based guided-wave circuit to form a 4 × 4 space switch has been reported [78]. Three switching paths with fiber-to-fiber losses around 30 dB have been shown and the importance of residual reflections has been pointed out. Toward this end, a polarization insensitive 4-SOA array operating at 1.3-μm wavelength with >20-dB gain on all channels has been reported [79].

To achieve low back reflections, facets of SOA's are often tilted by 7°–10°. Application of a tilt in a 4-SOA module with angle polished fibers resulted in uniform fiber-to-fiber gain of 14 ± 1 dB for all channels, low-gain ripple of ± 0.1 dB and a fairly low-polarization sensitivity of 2 dB [80], [81]. Assembly has been performed using the silicon-based V-grooves for self alignment of fibers and SOA-array. Fig. 14 shows the uniform gain characteristics of the used 4-SOA array measured between lensed fibers for TE and TM polarizations.

Drawbacks of this configuration with polished fibers are large coupling losses due to the large mode mismatches. Lensed fibers promise lower coupling losses but more stringent alignment tolerances as well. The concept of angle polishing to maintain parallel facets of fibers and SOA chip is not possible anymore unless further mode adaption is performed on the SOA chip. Accurate control of assembly angle with lensed fibers in the realization of a 4-SOA module recently resulted in 17 ± 3-dB fiber-to-fiber gain as given in Fig. 15 [82].

Table IV summarizes selected SOA-based space switches.

Main drawback of SOA's used for space switching application in WDM environments is the gain variation with injected

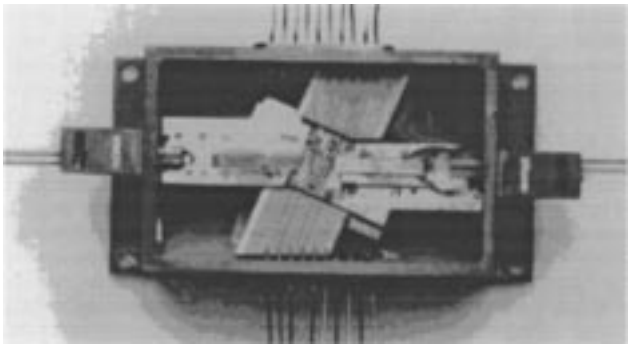

Fig. 15. Photograph of the 4-SOA array module [82].

TABLE IV
A SELECTION OF PUBLISHED SOA SPACE SWITCHES ON III–V SEMICONDUCTOR

Matrix Type	Switch points	Material	Results	Ref / year
2x2	4 SOA	InGaAsP	λ = 1.55 μm, TE, fib-fib loss 12 dB, current 100 mA, on/off > 40 dB	[65] 1992
2x2 + lasers	4 SOA + lasers	InGaAs/ InGaAsP MQW	λ = 1.55 μm, TE, out-power 0.8 W, current 70 + 50 mA, on/off > 12 dB	[66] 1992
2x2	4 SOA	InGaAsP	λ = 1.3 μm, TE, fib-fib gain 9 - 13 dB current 150 mA, on/off > 30 dB, switching time < 1ns	[83] 1992
2x2	4 SOA + mirrors	InGaAsP	λ = 1.55 μm, TE & TM ±2 dB, fib-fib gain up to 6 dB, current 200 mA, on/off 45 dB	[67] 1994
2x2	6 SOA in 2 stages	InGaAsP	λ = 1.28 μm, fib-fib gain > 0 dB, current 75 + 60 mA	[68] 1995
2x2	4 SOA	InGaAsP	λ = 1.58 μm, TE & TM ±3 dB, fib-fib gain up to 7 dB, current 160 mA, on/off 25 dB	[69] 1996
2x2	4 SOA + 8 TIR	InGaAsP	λ = 1.3 μm, fib-fib gain up to 1 dB, current 80 + 250 mA, on/off >40dB	[76] 1993
1x4	4 SOA	InGaAsP	λ = 1.57 μm, TE, fib-fib gain > 0 dB, current 58 mA, on/off 38 dB	[70] 1996
4x4 Benes	SOA	InGaAs/ GaAs QW	λ = 0.99 μm, fib-fib gain > 0 dB, current 16 mA typ., on/off > 30 dB switch time < 1ns	[75] 1992
4x4	16 SOA + 32 TIR	InGaAsP	λ = 1.3 μm, TE & TM ±1 dB, fib-fib gain up to 5 dB, current 250 + 120mA, on/off 54 dB	[77] 1994
4x4	24 SOA (3 stages)	InGaAsP	λ = 1.55 μm, TE, fib-fib gain up to 6 dB, current 50 + 50 + 100mA, on/off 40 dB	[71] 1992
4x4	24 SOA (3 stages)	InGaAsP	λ = 1.55 μm, TE & TM ±0.5 dB, fib-fib gain up to 0 dB, current 20 + 20 + 50 mA, on/off 40 dB	[72] 1995
4-Array	4 SOA	InGaAsP	λ = 1.31 μm, TE & TM ±0.5 dB, chip gain 20 dB, current 100 mA	[79] 1994
4x4 module	hybrid 2x8-array SOA	InGaAsP SiO2/TiO2	λ = 1.3 μm, insertion loss ≥ 26 dB, current 80 mA, on/off 30 dB	[78] 1992
4-Array Module	4 SOA	InGaAsP	λ = 1.55 μm, TE & TM ±1 dB, fib-fib gain 14 ± 1 dB, current 80 mA	[80,81] 1995
4-Array Module	4 SOA	InGaAsP	λ = 1.55μm, fib-fib gain 17.3 ± 3 dB, current 150 mA	[82] 1996

signal which is inherent to traveling-wave SOA's due to the modulation of the carrier concentration. The gain of almost 30 dB at 200-mA injected current for low-input signal powers (Fig. 16) is reduced with increasing signal power. The gain is reduced by 3 dB at an output saturation power of 9.5 dBm in this case (Fig. 17).

Gain varies with injected power in very short times of <1 ns. The gain variations therefore transform into signal distortion and reduction of on–off ratios of modulated signals as well as into crosstalk due to cross-gain modulation for WDM signals with several modulated wavelength channels.

Recently, gain clamping with an internal laser oscillation in order to block the carrier concentration at lasing threshold has

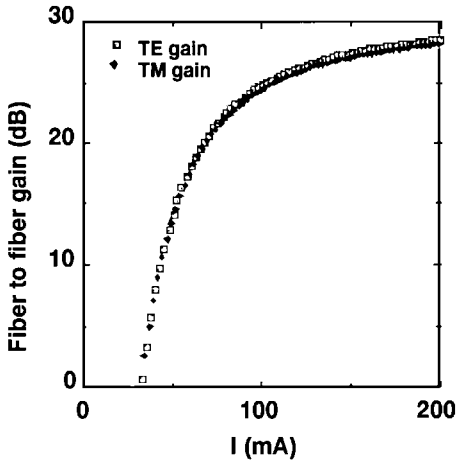

Fig. 16. Gain as function of injected current for traveling-wave SOA.

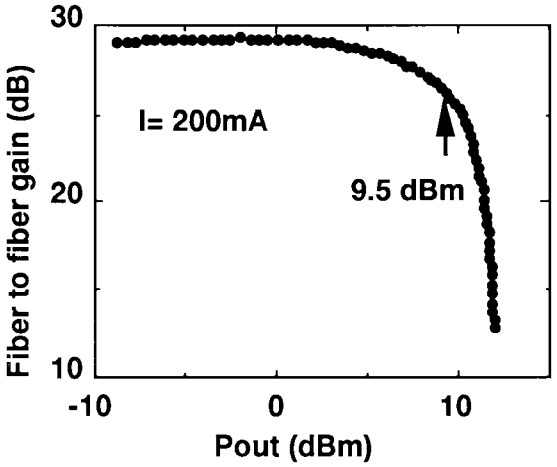

Fig. 17. Gain as function of injected light power for traveling-wave SOA.

been proposed. In addition to the DFB (distributed feedback) configuration [84]–[86], the DBR (distributed Bragg reflector) arrangement has been tested with external diffraction gratings [87] or fiber gratings [88]. A monolithic version for TE-polarization at 1.3-μm wavelength has been demonstrated for cable television (CATV) applications [89]. For the 1.55-μm wavelength range, a polarization insensitive monolithically integrated clamped-gain SOA has been reported [90].

Devices consist of three sections: a central gain section, passive sections at input and output with DBR gratings for wavelength selective feedback and large-mode size for efficient fiber-chip coupling, and mode size adaptors between active and passive sections. The considered DBR-based clamped-gain SOA is schematically shown in Fig. 18. Overall device length is 1 mm. Waveguides are tilted by 7°, with respect to the cleavage planes and antireflection coated to achieve low reflections in the range of 10^{-4}.

Fiber-to-fiber gain as shown in Fig. 19 increases for increasing driving current up to the lasing threshold of 50 mA, where gain is clamped at 14 dB with less than 0.5-dB polarization dependence. Lasing wavelength and gain peak are located at 1508 and 1538 nm, respectively and gain ripple is negligible (<0.2 dB). Gain is constant up to an output power of +12

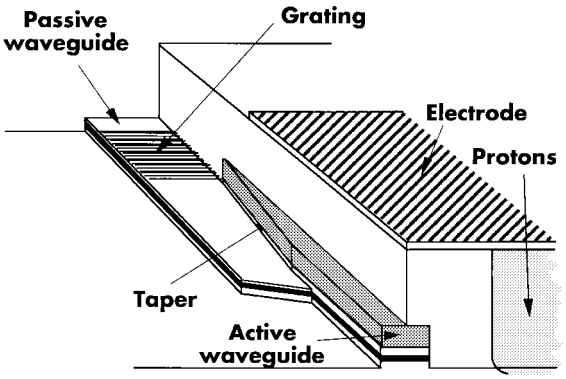

Fig. 18. Monolithically integrated DBR-based clamped-gain SOA for the 1.55-μm wavelength window [90].

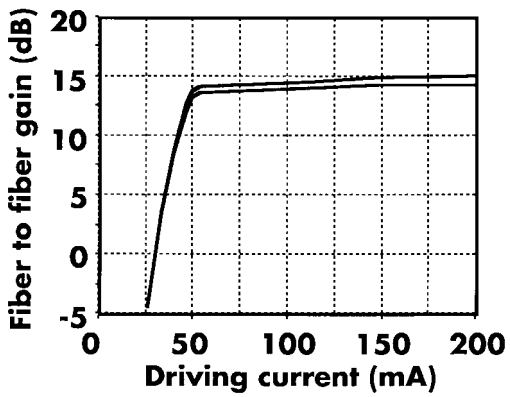

Fig. 19. Fiber-to-fiber gain of SOA clamped at 14 dB with less than 0.5-dB polarization sensitivity as shown by the two curves [90].

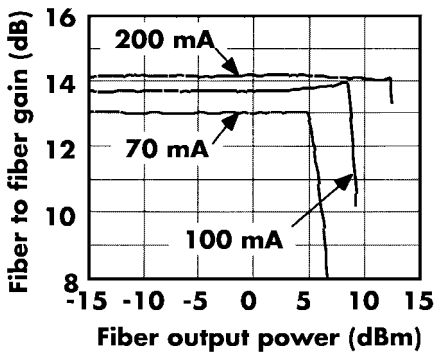

Fig. 20. Gain at 200-mA injected current is constant up to +12-dBm output power.

dBm at 200-mA injected current (Fig. 20). Switching times are below 1 ns.

The realized clamped-gain SOA's are well suited for WDM signals, since gain varies only 1 dB in a wavelength range of 25 nm (Fig. 21).

Devices have been tested in a 4 $\times$ 4 switch configuration, where they amplify and route 16 WDM channels [91]. The large available power range permits simultaneous amplification and routing of 16 channels modulated at 10 Gb/s with penalties below 1 dB for a remaining power range of 6 dB for all 16 channels. Fig. 22 shows the amplified 16 $\times$ 10 Gb/s WDM signal.

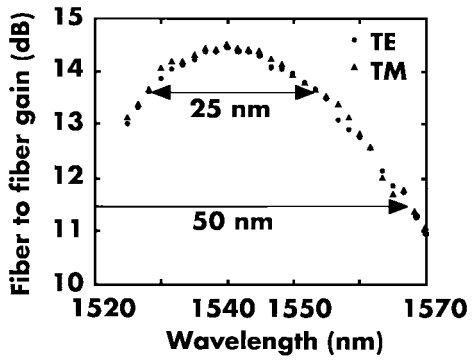

Fig. 21. Gain variation of clamped-gain SOA with wavelength.

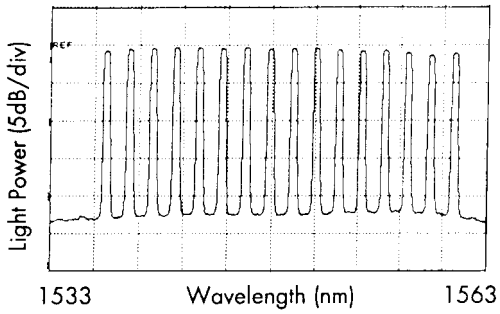

Fig. 22. Spectrum of amplified 16 $\times$ 10 Gb/s WDM signal [91].

V. Discussion of Space Switch Structures

We have reviewed the state of the art of passive and active space switches on III–V semiconductor material in the research community. Both passive and active switches realized on III–V semiconductors offer fast reconfiguration time and monolithic integration which are essential characteristics. Fast reconfiguration times in the nanosecond range are compulsory for packet switching applications [92]. In the microsecond range, it can be an attractive feature also for OADM's and OXC's as it allows to reconfigure in a short time the connections in the network and therefore eases the protection schemes (in case of fiber break for example). Advantages of passive switches are the transparency to the bit rate and their low noise. A major drawback of losses can be overcome by active switches that offer gain but not unlimited bit rate. Both passive and active configurations can be interesting according to the applications. Promising examples of passive switches are MZI and DOS mainly thanks to their easier control of fabrication as compared to directional couplers. DOS offer digital response and therefore polarization independence but require larger refractive index changes whereas MZI switches are more difficult to make polarization independent but offer higher speed by using electrooptical effects. Active switches are most promising thanks to light amplification especially when the concept of gain clamping is used to overcome signal distortion and cross gain modulation of WDM signals.

The implementation in the future optical networks will also strongly depend on considerations like manufacturability, fabrication yield, reliability and cost effectiveness. As far as manufacturability is concerned, most of these devices essentially exploit technologies which are already in production

for emitters and receivers (epitaxy, etching, ion implantation, dielectrics, metallizations, etc.). In addition, for similar growth, fabrication, and packaging complexity, the smaller size components will tend to be lower cost and higher yield. Reliability issue has only been recently reported on DOS [93] without any short term degradation. The SOA structures are very close to laser ones and are expected to have similarly good reliability. To build large switching matrices, integration is essential and combination of monolithic and hybrid technologies will probably be necessary. In this context, the packaging will be a critical issue that will require further development of mode adapters and assembly procedures.

VI. Conclusion

This paper has reviewed the various optical space switch structures on III–V semiconductors, which offer high potential for monolithic integration and compatibility with fabrication tools already used to manufacture optoelectronic components. The characteristics of directional couplers, Mach–Zehnder interferometers, digital optical switches, and semiconductor optical amplifier space switches have been discussed in the context of WDM optical transport and switching network applications, both in terms of performances and other criteria, such as size and fabrication tolerance, which are also key parameters for field implementation of space switch matrices.

Acknowledgment

The authors would like to thank their colleagues in the Photonic Network Unit, in particular, D. Chiaroni, A. Jourdan, P. Perrier, and M. Sotom for the system architectures and system results mentioned here.

References

[1] P. A. Perrier, S. Ruggeri, C. Coeurjolly, A. Noury, P. Gavignet, S. Gauchard, V. Havard, L. Berthelon, H. Février, and J. Dupraz, "4-channel, 10 Gb/s capacity self-healing WDM ring network with wavelength add/drop multiplexers," in *OFC'96*, San Jose, CA, Feb. 25–Mar. 1, 1996, pp. 218–220.

[2] G. Tobolka, "The EU-ACTS PHOTON project," presented at the International Workshop on Photonic Networks and Technologies, Lerici, Italy, Sept. 3–6, 1996.

[3] A. Jourdan, F. Masetti, M. Garnot, G. Soulage, and M. Sotom, "Design and implementation of a fully reconfigurable all-optical crossconnect for high capacity multi-wavelength transport networks," *J. Lightwave Technol.*, vol. 14, pp. 1198–1206, June 1996.

[4] A. Jourdan, G. Soulage, S. Artigaud, K. Wünstel, P. Doussière, M. Bachmann, J. Da Laura, F. Bruyère, and M. Sotom, "WDM networking experiment including all-optical crossconnect cascade and transmission over 320 km G.652 fiber at up to 10 Gb/s," in *ECOC'96*, Oslo, Norway, Sept. 15–19, 1996, pp. 4.123–4.126.

[5] D. Chiaroni, C. Chauzat, D. De Bouard, S. Gurib, M. Sotom, J. M. Gabriagues, "A novel photonic switching architecture for high capacity ATM switching applications," presented at Photonics in Switching'95, Salt Lake City, UT, Mar. 1995, paper PThC3.

[6] D. Chiaroni, C. Chauzat, D. De Bouard, and M. Sotom, "Sizeability analysis of a high speed photonic packet switching architecture," in *ECOC'95*, Brussels, Belgium, Sept. 17–21, 1995, pp. 793–796.

[7] M. Tachikura, T. Katagiri, and H. Kobayashi, "Strictly nonblocking 512 × 512 optical fiber matrix switch based on three-stage clos network," *IEEE Photon. Technol. Lett.*, vol. 6, pp. 764–766, June 1994.

[8] P. Granestrand, B. Lagerström, P. Svensson, H. Olofsson, J.-E. Falk, and B. Stolz, "Pigtailed tree-structured 8 × 8 $LiNbO_3$ switch matrix with 112 digital optical switches," *IEEE Photon. Technol. Lett.*, vol. 6, pp. 71–73, Jan. 1994.

[9] E. Murphy, T. O. Murphy, A. F. Ambrose, R. W. Irvin, B. H. Lee, P. Peng, G. W. Richards, and A. Yorinks, " 16 × 16 nonblocking guided-wave optical switching system," *J. Lightwave Technol.*, vol. 14, pp. 352–358, Mar. 1996.

[10] P. J. Duthie and M. J. Wale, "A 16 × 16 single chip optical switch array in lithium niobate," *Electron. Lett.*, vol. 27, no. 14, pp. 1265–1266, 1991.

[11] JH. Okayama and M. Kawahara, "Prototype 32 × 32 optical switch matrix," *Electron. Lett. 7*, vol. 30, no. 14, pp. 1128–1129, July 7, 1994.

[12] A. Himeno, T. Goh, M. Okuno, H. Takahashi, and K. Hattori, "Silica-based low loss and high extinction ratio 8 × 8 thermo-optic matrix switch with path independent loss arrangement using double Mach Zehnder interferometer switching units," in *ECOC'96*, Oslo, Norway, pp. 4.149–4.152, paper ThD.2.2.

[13] A. Borreman, T. Hoekstra, M. Diemer, H. Hoekstra, and P. Lambeck, "Polymeric 8 × 8 digital optical switch matrix," in *ECOC'96*, Oslo, Norway, pp. 5.59–5.62, postdeadline paper ThD.3.2.

[14] R. Moosburger, E. Brose, G. Fishbeck, C. Kostrzewa, B. Schüppert, and K. Pettermann, "Robust digital optical switch based on a novel patterning technique for oversized polymer rib waveguides," in *ECOC'96*, Oslo, Norway, pp. 2.67–2.70, Paper ThC.1.5.

[15] D. J. Blumenthal and L. Thylen, "Coherent crosstalk induced BER floors in $N \times N$ space photonic switches," *IEEE/LEOS Summer Top. Meet. Optical Networks and Their Enabling Technologies*, Lake Tahoe, NV, July 11–13, 1994, postdeadline paper.

[16] Y. Bourbin, A. Enard, R. Blondeau, M. Razeghi, D. Rondi, M. Papuchon, and B. De Cremoux, "Electro-optical modulators using novel buried waveguides in GaInAsP material," *Electron. Lett.*, vol. 24, pp. 221–222, 1988.

[17] J. E. Goell, "Rib waveguide for integrated optical circuits," *Appl. Opt.*, vol. 12, pp. 2297–2298, 1973.

[18] N. Yoshimoto, Y. Shibata, S. Oku, S. Kondo, Y. Noguchi, K. Wakita, K. Kawano, and M. Naganuma, "Full polarization insensitive Mach–Zehnder optical switches using a wide-well InGaAlAs/InAlAs MQW structures," *Photonics in Switching*, Sendai, Japan, Apr. 21–25, 1996, pp. 78–79.

[19] Y. Bourbin, A. Enard, R. Blondeau, D. Rondi, and M. Papuchon, "Very low loss and efficient modulators in InGaAsP/InP," in *IGWO'89*, Houston, TX, Feb. 6–8, 1989, p. 110.

[20] J. H. Angenent, M. Erman, J. M. Auger, and R. Gamonal, "Extremely low loss InP/ GaInAsP rib waveguides," *Electron. Lett.*, vol. 25, p. 628, 1989.

[21] R. C. Alferness, "Waveguide electro-optic modulators," *IEEE Trans. Microwave Theory Tech.*, vol. MTT-30, pp. 1121–1137, 1982.

[22] D. A. B. Miller, D. S. Chemla, T. C. Damen, A. C. Gossard, W. Wiegemann, T. H. Wood, and C. A. Burrus, "Band-edge electroabsorption in quantum well structures: The quantum confined stark effect," *Phys. Rev. Lett.*, vol. 53, pp. 2173–2176, 1984.

[23] J. E. Zucker, K. L. Jones, T. H. Chiu, B. Tell, and K. Brown-Goebeler, "Strained quantum wells for polarization-independent electrooptic waveguide switches," *J. Lightwave Technol.*, vol. 10, pp. 1926–1929, Dec. 1992.

[24] J. F. Vinchant, J. A. Cavaillès, M. Erman, P. Jarry, and M. Renaud, "InP/GaInAsP guided wave phase modulators based on carrier induced effects: Theory and experiment," *J. Lightwave Technol.*, vol. 10, pp. 63–70, 1992.

[25] J. H. Angenent, M. Erman, M. Renaud, C. Graver, J. M. Auger, R. Gamonal, J. A. Cavaillès, and P. Thijs, "Optical switches on InP substrate using carrier depletion with driving voltages as low as 4.5 Volt," presented at ECOC'89, Gothenborg, Sweden, Sept. 11–14, 1989, paper WeA13-3.

[26] M. Renaud, I. Privat, J. P. Hébert, J. Le Bris, J. L. Peyre, A. Pinquier, and J. F. Vinchant, "High speed multifunctional InP module for optical signal processing," presented at ECOC'94, Firenze, Italy, Sept. 25–29, 1994.

[27] K. Tada and K. Hirose," A new light modulator using perturbation of synchronism between two coupled guides," *Appl. Phys. Lett.*, vol. 25, pp. 561–562, 1974.

[28] M. Erman, "InP optoelectronic devices and photonic integrated circuits for high speed packet switching," in *Photonic Switching Conf.*, Minsk, July 1–3, 1992.

[29] E. Lallier, A. Enard, D. Rondi, G. Glastre, R. Blondeau, M. Papuchon, and N. Vodjani, "InGaAsP/InP 4 × 4 optical switch matrix with current injection tuned directional couplers," in *ECOC/IOOC*, Paris, France, 1991, pp. 44–47.

[30] P. J. Duthie, N. Shaw, M. Wale, and I. Bennion, "Guided wave switch array using electro-optic and carrier depletion effects in Indium Phosphide," *Electron. Lett.*, Vol. 27, no. 19, pp. 1747–1748, 1991.

[31] K. Hamamoto, T. Anan, K. Komatsu, M. Sugimoto, and I. Mito, "First 8 × 8 semiconductor optical matrix switches using GaAs/GaAlAs directional couplers," *Electron. Lett.*, Vol. 28, pp. 441–443, 1992.

[32] L. Stoll, G. Müller, M. Honsberg, M. Schienle, J. Eichinger, and U. Wolf, "4 × 4 optical matrix switch on InP with low switching current," *AEO*, vol. 46, pp. 116–118, 1992.

[33] H. Takeuchi, Y. Hasumi, K. Kondo, and Y. Noguchi, "4×4 directional coupler switch matrix with an InGaAlAs/InAlAs multiple quantum well structure," *Electron. Lett.*, vol. 29, no. 6, p. 523, Mar. 18, 1993.

[34] D. Hoffmann, C. Bornholdt, F. Kappe, L. Mörl, and F.-W. Reier, "Novel digital optical switch with crosstalk below -40 dB based on absorptive switching," in *ECOC'95*, Brussels, Belgium, Sept. 17–21, pp. 107–110.

[35] L. Stoll, G. Müller, U. Wolff, B. Sauer, S. Eichinger, and S. Sürgeç, "Compact and polarization independent optical switch on InP/InGaAsP," in *Proc. Eur. Conf. Optical Communication (ECOC)*, Berlin, Germany, 1992, pp. 337–340.

[36] F. Zernike, "Integrated optics switch," *Dig. Top. Meet. Integrated Optics*, New Orleans, LA, 1974, pp. 1–4, paper WA5.

[37] W. E. Martin, "A new waveguide switch/modulator for integrated optics," *Appl. Phys. Lett.*, vol. 26, pp. 562–564, 1975.

[38] Y. Ohmachi and J. Noda, "Electro-optic light modulator with branched ridge waveguide," *Appl. Phys. Lett.*, vol. 27, pp. 544–546, 1975.

[39] P. Buchmann, H. Kaufmann, H. Melchior, and G. Guekos, "Broadband Y-branch electro-optic GaAs waveguide interferometer for 1.3 μm," *Appl. Phys. Lett.*, vol. 46, pp. 462–464, 1985.

[40] M. Bachmann, M. K. Smit, P. A. Besse, E. Gini, H. Melchior, and L. B. Soldano, "Polarization-insensitive low-voltage optical waveguide switch using InGaAsP/InP four-port Mach–Zehnder interferometer," in *Proc. Conf. Opt. Fiber Commun. (OFC)*, San Jose, CA, 1993, pp. 32–33.

[41] P. A. Besse, M. Bachmann, and H. Melchior, "Phase relations in multimode interference couplers and their application to generalized integrated Mach-Zehnder optical switches," in *Proc. Eur. Conf. Integrated Optics (ECIO)*, Neuchâtel, Switzerland, 1993, pp. 2.22–2.23.

[42] L. B. Soldano and E. C. M. Pennings, "Optical multimode interference devices based on self-imaging: Principles and applications," *J. Lightwave Technol.*, vol. 13, no. 4, pp. 615–627, 1995.

[43] M. Bachmann, P. A. Besse, and H. Melchior, "General self-imaging properties in $N \times N$ multi-mode interference couplers including phase relations," *Appl. Opt.*, vol. 33, pp. 3905–3911, 1994.

[44] ———, "Overlapping-image multi-mode interference couplers with reduced number of self-images for uniform and nonuniform power splitting," *Appl. Opt.*, vol. 34, pp. 6898–6910, 1995.

[45] M. Bachmann, E. Gini, and H. Melchior, "Polarization-insensitive waveguide modulator using InGaAsP/InP Mach–Zehnder interferometer," in *Proc. Eur. Conf. Optical Communication (ECOC)*, Berlin, Germany, 1992, pp. 345–348.

[46] R. Krähenbühl, M. Bachmann, W. Vogt, T. Brenner, H. Duran, R. Bauknecht, W. Hunziker, R. Kyburz, Ch. Holtmann, E. Gini, and H. Melchior, "High-speed low-loss InP space switch matrix for optical communication systems, fully packaged with electronic drivers and single-mode fibers," in *Proc. Eur. Conf. Optical Communication (ECOC)*, Firenze, Italy, 1994, pp. 511–514.

[47] R. Krähenbühl, R. Kyburz , W. Vogt, M. Bachmann, T. Brenner, E. Gini, and H. Melchior, "Low-loss polarization-insensitive InP / InGaAsP optical space switches for fiber optical communication," *IEEE Photon. Technol. Lett.*, vol. 8, pp. 632–634, June 1996.

[48] N. Agrawal, C. M. Weinert, H.-J. Ehrke, G. G. Mekonnen, D. Franke, C. Bornholdt, and R. Langenhorst, "Fast 2 × 2 Mach–Zehnder optical space switches using InGaAsP–InP multiquantum-well structures," *IEEE Photon. Technol. Lett.*, vol. 7, pp. 644–645, June 1995.

[49] F. Kappe, G. G. Mekonnen, C. Bornholdt, F. W. Reier, and D. Hoffman, "35 GHz bandwidth photonic space switch with travelling wave electrodes on InP," *Electron. Lett.*, vol. 30, no. 13, pp. 1048–1049, 1994.

[50] R. M. Jenkins, J. M. Heaton, D. R. Wight, J. T. Parker, J. C. H. Birbeck, G. W. Smith, and K. P. Hilton, "Novel $1 \times N$ and $N \times N$ integrated optical switches using self-imaging multimode GaAs/AlGaAs waveguides," *Appl. Phys. Lett.*, vol. 64, pp. 684–686, 1994.

[51] M. Bachmann, C. Nadler, P. A. Besse, and H. Melchior, "Compact polarization-insensitive multi-leg 1 × 4 Mach–Zehnder switch in InGaAsP/InP," in *Proc. Eur. Conf. Optical Communication*, Firenze, Italy, 1994, pp. 519–522.

[52] Y. Silberberg, P. Perlmutter, and J. E. Baran, "Digital optical switch," presented at the Int. Conf. Optical Fiber Communication, 1988, paper ThA3.

[53] J. F. Vinchant, M. Renaud, A. Goutelle, M. Erman, P. Svensson, and L. Thylén, "Low driving voltage or current digital optical switch on InP for multi-wavelength system applications," *Electron. Lett.*, vol. 28, no. 12, pp. 1135–1136, 1992.

[54] J. A. Cavaillès, M. Renaud, J. F. Vinchant, M. Erman, P. Svensson, and L. Thylén, "First digital optical switch based on InP/GaInAsP double heterostructure waveguides," *Electron. Lett.*, vol. 27, no. 9, pp. 699–700, 1991.

[55] J. F. Vinchant, M. Renaud, M. Erman, J. L. Peyre, P. Jarry, and P. Pagnod Rossiaux, "InP digital optical switch: Key element for guided wave photonic switching," *Proc. Inst. Elect. Eng.*, pt. J, vol. 140, no. 5, Oct. 1993.

[56] J. F. Vinchant, M. Renaud, A. Goutelle, J. L. Peyre, P. Jarry, M. Erman, P. Svensson, and L. Thylén, "First polarization insensitive 4 × 4 switch matrix on InP with digital optical switches," in *ECOC'92*, Berlin, Germany, 1992, pp. 341–344.

[57] J. F. Vinchant, A. Goutelle, B. Martin, F. Gaborit, P. Pagnod Rossiaux, J. L. Peyre, J. Le Bris, and M. Renaud, "New compact polarization insensitive 4 × 4 switch matrix on InP with digital optical switches and integrated mirrors, " presented at ECOC'93, Montreux, Switzerland, 1993, post-deadline paper.

[58] A. Jourdan, G. Soulage, G. Da Loura, B. Clesca, P. Doussière, C. Duchet, D. Leclerc, J. F. Vinchant, and M. Sotom, "Experimental assessment of a 4 × 4, 4 wavelength all-optical cross- connect at 10 Gb/s line rate," presented at the Int. Conf. Optical Fiber Communication, 1995.

[59] M. N. Kahn, J. E. Zucker, L. L. Buhl, B. I. Miller, and C. A. Burus, "Fabrication-tolerant, low loss and high speed digital optical switches in InGaAsP/InP quantum wells," in *ECOC'95*, Brussels, Belgium, vol. 1, Sept. 17–21, 1995, pp. 103–106.

[60] W. H. Nelson, A. N. M. Masum Choudhoury, M. Abbdalla, R. Bryant, E. Meland, and W. Niland, "Wavelength and polarization independent large angle InP/InGaAsP digital optical switches with extinction ratios exceeding 20 dB," *IEEE Photon. Technol. Lett.*, vol. 6, pp. 1332–1334, Nov. 1994.

[61] M. Renaud, J. F. Vinchant, A. Goutelle, B. Martin, G. Ripoche, M. Bachmann, P. Pagnod, and F. Gaborit, "Compact digital optical switches for low insertion loss large switch arrays on InP," in *ECOC'95*, Brussels, Belgium, vol. 1, Sept. 17–21, 1995, pp. 99–102.

[62] H. P. Nolting, M. Gravert, M. Bachmann, and M. Renaud, "Crosstalk reduced digital optical switch with single electrode designed for InP," in *IPR'96 Conf.*, Boston, MA, pp. 637–640, paper IThC4–1.

[63] M. Bachmann, M. Renaud, H. P. Nolting, and M. Gravert, " Crosstalk reduced DOS with high fabrication tolerances designed for InGaAsP/InP," in *ECOC'96*, Oslo, Norway, 1996, pp. 3.261–3.264.

[64] P. Doussière, "Recent advances in conventional and gain clamped semiconductor optical amplifiers," presented at Conf. Optical Amplifiers and Their Applications (OAA), 1996, invited paper.

[65] M. Janson, L. Lundgren, A.-C. Mörner, M. Rask, B. Stoltz, M. Gustavsson, and L. Thylén, "Monolithically integrated 2 × 2 InGaAsP/InP laser amplifier gate switch arrays," *Electron. Lett.*, vol. 28, no. 8, pp. 776–778, 1992.

[66] M. G. Young, U. Koren, B. I. Miller, M. Chien, M. A. Newkirk, and J. M. Verdiell, "A compact 2×2 amplifier switchted DBR lasers operating at 1.55 μm," *IEEE Photon Technol. Lett.*, vol. 4, pp. 1046–1048, Sept. 1992.

[67] G. Sherlock, J. D. Burton, P. J. Fiddyment, P. C. Sully, A. E. Kelly, and M. J. Robertson, "Integrated 2 × 2 optical switch with gain," *Electron. Lett.*, vol. 30, no. 2, pp. 137–138, 1994.

[68] K. Hamamoto and K. Komatsu, "Insertion-loss-free 2 × 2 InGaAsP/InP optical switch fabricated using bandgap energy controlled selective MOVPE," *Electron. Lett.*, vol. 31, no. 20, pp. 1779–1781, 1995.

[69] F. Dorgeuille, B. Mersali, M. Feuillade, S. Sainson, J. Brandon, S. Slempkès, and M. Carré, "Monolithic InGaAsP-InP tapered laser amplifier gate 2 × 2 switch matrix with gain," *Electron. Lett.*, vol. 32, no. 7, pp. 686–688, 1996.

[70] K. Hamamoto, T. Sasaki, T. Matsumoto, and K. Komatsu, "Insertion-loss-free 1 × 4 optical switch fabricated using bandgap-energy-controlled selective MOVPE," in *ECOC'96*, Oslo, Norway, 1996, pp. 4.153–4.156.

[71] M. Gustavsson, B. Lagerström, L. Thylén, M. Janson, L. Lundgren, A.-C. Mörner, M. Rask, and B. Stoltz, "Monolithically integrated 4 × 4 InGaAsP/InP laser amplifier gate switch arrays," *Electron. Lett.*, vol. 28, no. 24, pp. 2223–2225, 1992.

[72] W. van Berlo, M. Janson, L. Lundgren, A.-C. Mörner, J. Terlecki, M. Gustavsson, P. Granestrand, and P. Svensson, "Polarization-insensitvie, monolithic 4 × 4 InGaAsP–InP laser amplifier gate switch matrix," *IEEE Photon. Technol. Lett.*, vol. 7, pp. 1291–1293, Nov. 1995.

[73] M. Gustavsson, M. Janson, and L. Lundgren,, "Digital transmission experiment with monolithically integrated 4 × 4 InGaAsP/InP laser

amplifier gate switch array," *Electron. Lett.*, Vol. 29, no. 12, pp. 1083–1085, 1993; correction vol. 29, no. 14, p. 1310, 1993.
[74] E. Almström, C. P. Larsen, L. Gillner, W. H. van Berlo, M. Gustavsson, and E. Berglind, "Experimental and analytical evaluation of packaged 4 × 4 InGaAsP/InP semiconductor optical amplifier gate switch matrices for optical networks," *J. Lightwave Technol.*, vol. 14, pp. 996–1004, June 1996.
[75] M. Ikeda, S. Oku, Y. Shibata, T. Suzuki, and M. Okayasu, "Lossless 4×4 monolithic LD optical matrix switches," in *SPIE, Photonic Switching*, vol. 1807, 1992, pp. 402–406.
[76] T. Kirihara, M. Ogawa, H. Inoue, and K. Ishida, "Lossless and low-crosstalk characteristics in an InP-based 2 × 2 optical switch," *IEEE Photon. Technol. Lett.*, vol. 5, pp. 1059–1061, Sept. 1993.
[77] T. Kirihara, M. Ogawa, H. Inoue, H. Kodera, and K. Ishida, "Lossless and low-crosstalk characteristics in an InP-based 4 × 4 optical switch with integrated single-stage optical amplifiers," *IEEE Photon. Technol. Lett.*, vol. 6, pp. 218–221, Feb. 1994.
[78] Y. Yamada, H. Terui, Y. Ohmori, M. Yamada, A. Himeno, and M. Kobayashi, "Hybrid-integrated 4 × 4 optical gate matrix switch using silica-based optical waveguides and LD array chips," *J. Lightwave Technol.*, vol. 10, pp. 383–389, Mar. 1992.
[79] S. Kitamura, K. Komatsu, and M. Kitamura, "Polarization-insensitive semiconductor optical amplifier array grown by selective MOVPE," *IEEE Photon. Technol. Lett.*, vol. 6, pp. 173–175, Feb. 1994.
[80] W. Hunziker, W. Vogt, H. Melchior, D. Leclerc, P. Brosson, F. Pommereau, R. Ngo, P. Doussière, F. Mallécot, T. Fillion, I. Wamsler, and G. Laube, "Self-aligned flip-chip of tilted semiconductor optical amplifier arrays on Si motherboard," *Electron. Lett.*, vol. 31, no. 6, pp. 488–490, 1995.
[81] D. Leclerc, P. Brosson, F. Pommereau, R. Ngo, P. Doussière, F. Mallécot, P. Gavignet, I. Wamsler, G. Laube, W. Hunziker, W. Volt, and H. Melchior, "High-performance semiconductor optical amplifier array for self-aligned packaging using Si V-groove flip-chip technique," *IEEE Photon. Technol. Lett.*, vol. 7, npp. 476–478, May 1995.
[82] J. Le Bris, M. Di Maggio, M. Goix, P. Brosson, M. Renaud, and E. Grard, "High performance semiconductor array module using tilted ribbon lensed fiber and dynamical alignement," in *ECOC'96*, Oslo, Norway, 1996, pp. 4.93–4.96.
[83] Ch. Holtmann, T. Brenner, R. Dall'Ara, P. A. Besse, and H. Melchior, "Monolithically integrated semiconductor optical amplifiers for transparent 2 × 2 switches at 1.3 micrometers," *AGEN-Mitteilungen*, no. 56/57, pp. 45–48, 1993.
[84] B. Bauer, F. Henry, and R. Schimpe, "Gain stabilization of a semiconductor optical amplifier by distributed feedback," *IEEE Photon. Technol. Lett.*, vol. 6, pp. 182–185, 1994.
[85] P. Doussière, A. Jourdan, G. Soulage, P. Garabédian, C. Graver, T. Fillion, E. Derouin, and D. Leclerc, "Clamped gain travelling wave semiconductor optical amplifier for wavelength division multiplexing applications," in *Semiconductor Laser Conf.*, Maui, HI, 1994, pp. 185–186.
[86] L. F. Tiemeijer, P. J. A. Thijs, T. V. Dongen, J. J. M. Binsma, E. J. Jansen, and H. R. J. R. van Helleputte, "Reduced intermodulation distortion in 1300 nm gain-clamped MQW laser amplifiers," *IEEE Photon. Technol. Lett.*, vol. 7, pp. 284–286, 1995.
[87] J. C. Simon, P. Doussière, P. Lamouler, I. Valiente, and F. RIou, "Travelling wave semiconductor optical amplifier with reduced nonlinear distortions," *Electron. Lett.*, vol. 30, pp. 49–50, 1994.
[88] Ch. Holtmann, P. A. Besse, H. Melchior, and D. L. Williams, "Gain-clamped semiconductor optical amplifier for 1.3 μm wavelength with 20 dB polarization independent fiber-to-fiber gain and significantly reduced pulse shape and intermodulation distortions," in *Eur. Conf. Optical Communication (ECOC)*, Brussels, Belgium, 1995, pp. 1031–1034.
[89] G. N. van den Hoven, L. F. Tiemeijer, P. J. A. Thijs, T. van Dongen, J. J. M. Binsma, and E. J. Jansen, "1310 nm DBR-type MQW gain-clamped semiconductor optical amplifiers with AM-CATV-grade linearity," *Conf. Optical Amplifiers and Their Applications (OAA)*, 1996, post-deadline paper PDP2.
[90] M. Bachmann, P. Doussière, J. Y. Emery, R. N'Go, F. Pommereau, L. Goldstein, G. Soulage, and A. Jourdan, "Polarization-insensitive clamped-gain SOA with integrated spot-size convertor and DBR-gratings for WDM applications at 1.55 μm wavelength," *Electron. Lett.*, to be published.
[91] G. Soulage, A. Jourdan, P. Doussière, M. Bachmann, J. Y. Emery, J. Da Loura, and M. Sotom, "4 × 4 space-switch based on clamped-gain semiconductor optical amplifiers in a 16 × 10 Gbit/s WDM experiment," presented at the Eur. Conf. Optical Communication (ECOC), Oslo, Norway, 1996, paper ThD.2.1.
[92] D. Chiaroni, D. De Bouard, P. Doussière, C. Chauzat, and M. Sotom, "High performance semiconductor optical amplifier gate for fast WDM packet switching," in *ECOC'95*, Brussels, Belgium, Sept. 17–21, 1995, pp. 115–118.
[93] J. F. Vinchant, V. Hornung, F. Le Du, G. Ripoche, and G. Gelly, "Preliminary stability study of InP/InGaAsP digital optical switches," presented at the Integrated Photonic Research Conf., IPR'95, Dana Point, CA.

Monique Renaud was born in Chateaudun, France on May 7, 1960. She received the engineer diploma and the Docteur 3e cycle thesis from Institut National des Sciences Appliquées, Lyon, France, in 1983 and 1985, respectively.

In 1985, she joined Laboratoires d'Electronique Philips, where her fields of interest were physics and technology of III–V semiconductor microelectronics and integrated optics. Since July 1991, she joined Alcatel Alsthom Recherche and has been engaged in research on InP based photonic switching devices. She is currently leading a group on components for routing and switching in the Photonic Component Unit. Over the past years, she was participating to several European collaborative projects (RACE and ESPRIT) including the RACE/OSCAR 1033 and RACE/ATMOS 2089. She is currently coordinating the ACTS AC043 project KEOPS (KEys to Optical Packet Switching). She has contributed to about 85 papers in international journals or conferences.

Maurus Bachmann was born 1961 in Switzerland. In 1986, he joined the Institute of Quantum Electronics at ETH Zürich where he received his Ph.D. degree 1995 on polarization insensitive optical waveguide switches.

He mainly worked on theory, design, fabrication, and characterization techniques of InGaAsP–InP based integrated optical components including polarization insensitive optical switches and passive integrated optical devices like multimode interference couplers. In 1995, he joined Alcatel Alsthom Recherche, France where he is presently engaged in research on digital opical switches and semiconductor optical amplifiers. He has participated within international projects such as RACE/OSCAR, RACE/ATMOS and ACTS/KEOPS. He has contributed to about 35 papers in international journals and conferences.

Marko Erman (M'84) was born in Ljubljana, Slovenia. He received the engineer diploma in 1978 from Ecole Polytechnique, Paris, France, a second engineer diploma in 1980 from Ecole Sup'erieure de T'el'ecommunications, Paris, France, the Docteur 3rd cycle thesis in 1982, and the Docteur es Sciences Physique degree in 1986, both from the University of Paris, France.

In 1982, he joined Laboratoires d'Electronique Philips, where his fields of interest were optical properties of III–V semiconductors, optical characterization techniques and integrated optics. In 1989, he became head of Exploratory Research Group, and in 1990, head of Professional Imaging Group. Since July 1991, he has been with Alcatel Alsthom Recherche where he is currently Head of the Photonic Components Units. He has contributed to about 120 papers in international journals or presentations at international conferences, and holds 14 patents. Over the past years, he has been largely involved in several European project (RACE and ESPRIT), acting in particular as prime contractor and project manager for several projetcs.

Dr. Erman has participated in various conference program commitees, including ECOC, OFC, IOOC, CLEO, PS. He is member of SPIE.